

physica **p** status **s** solidi **S**

www.pss-journals.com

reprint



Calculated vibration spectrum of monoclinic Cu_2SnSe_3 in comparison with kesterite-type $\text{Cu}_2\text{ZnSnSe}_4$

Andrei V. Postnikov* and Narjes B. Mortazavi Amiri

LCP-A2MC, University of Lorraine, 1 Bd Arago, 57078 Metz, France

Received 10 October 2012, revised 8 March 2013, accepted 14 March 2013

Published online 3 June 2013

Keywords first-principles DFT calculations, phonons, photovoltaic materials

* Corresponding author: e-mail andrei.postnikov@univ-lorraine.fr, Phone: +33-387-315873, Fax: +33-387-315801

Frozen-phonon calculations on structurally related tetragonal $\text{Cu}_2\text{ZnSnSe}_4$ and monoclinic Cu_2SnSe_3 reveal similarities in the shape and overall composition of vibration spectra, but also marked deviations in the frequency and nature of certain modes. These deviations are often induced by different connectivity on the cation sublattice and can be traced to a specific structural

motive. In the analysis of vibrations, a variety of projection schemes applied to phonon eigenvectors calculated within the density functional theory by the SIESTA method help to reveal different aspects in vibration modes, *e.g.*, strength of particular in-phase atomic movements, or attribution of specific vibration modes to particular irreducible representations of the space group.

© 2013 WILEY-VCH Verlag GmbH & Co. KGaA, Weinheim

1 Introduction Phase diagram of CuZnSnSe system contains, along with kesterite-type $\text{Cu}_2\text{ZnSnSe}_4$ (CZTSe), a promising material for photovoltaic applications, secondary phases with high stability but inferior photovoltaic characteristics [1]. Discrimination of such phases by X-ray diffraction is complicated by the closeness of their underlying structures (generally a zincblende structure with different cation arrangements). However, vibration spectra, sensitive to *local* environments and *long-range* structural patterns, may be useful in identifying different phases. First-principle calculations can serve as important benchmarks for such identification. Earlier we compared kesterite- and stannite-type CZTSe (8 atoms per unit cell in each) in view of their different vibrational properties [2]. Recently, the monoclinic Cu_2SnSe_3 secondary phase (CTSe), which has four formula units, *i.e.*, 24 atoms, per unit cell, became subject to a detailed comparison with kesterite-type CZTSe [3]. In the present contribution, we expand this analysis over symmetry attribution to different modes, that helps to identify Raman- and infrared-silent ones. In a more broad context, we overview ways of post-processing the phonon calculations results on large systems, aimed at extracting useful information by different projection techniques.

2 Calculation details Vibration modes were extracted in a frozen phonons scheme, applied at the center of the

Brillouin zone (BZ) of the compound in question. Unless special efforts taken, longitudinal optical modes are not sampled. When dealing with a complex semiconductor superlattice, however, the BZ-center modes include folded branches from BZ boundary of the underlying zincblende aristotype, whose longitudinal character is then fully represented. The force constants follow from a sequence of finite-displacement calculations (of each atom individually in \pm three Cartesian directions out of equilibrium), without imposing any symmetry constraints. The necessary “machinery” is provided by the SIESTA calculation method [4, 5]. Technical aspects of calculation for both systems are given in Refs. [2, 3]. We specify only that the calculations used the local density approximation for the exchange-correlation, norm-conserving Troullier–Martins pseudopotentials with valence states starting from Cu/Zn/Se3d and In4d, and atom-centered numerical basis functions.

2.1 Total density of modes The results of phonon calculations are discrete eigenvalues ω_i and eigenvectors A_i^α of $i = 1, \dots, 3N$ vibration modes (N is the number of atoms in the unit cell; α number of atoms). The (i, α) component of A remains a vector in three-dimensional space of Cartesian displacements. A rather straightforward way to characterize these results is via the density of modes, which may be resolved into contributions from atoms within a given

species \mathbb{N} :

$$I_{\mathbb{N}}(\omega) = \sum_i \sum_{\alpha \in \mathbb{N}} |A_i^\alpha|^2 \delta(\omega - \omega_i). \quad (1)$$

Here, $\delta(\omega)$ is the δ -function for a genuinely discrete spectrum, but it is often practical to use, instead, a somehow broadened approximation. The corresponding densities of modes for both systems are shown in Fig. 1. Each plot shows two groups of peaks, separated by a gap centered at about 125 cm^{-1} , the upper group being cut at about 240 cm^{-1} . In CTSe, both groups are much broader – a mere consequence of a larger unit cell in this compound, whereby more modes which would have been off-zone-center in underlying zincblende structure are folded onto $\mathbf{q} = 0$ of the correspondingly reduced BZ.

2.2 Symmetry-projected density of modes The symmetry analysis of modes helps to judge which of them are Raman or infrared active, or otherwise sort out the modes depending on the conditions of experiment. Such analysis can be done *a priori*, using the symmetry coordinates generated according to different irreducible representations (IrReps) of the space group in question in place of bare Cartesian ones, and diagonalizing each symmetry block of the dynamical matrix independently. Alternatively, the analysis can be done *a posteriori*, using the projections of

Table 1 Decomposition of vibration modes in the CZTSe structure (space group $I\bar{4}$) according to symmetries.

Wyckoff positions	irred. representations			modes counting (sums up to 8 at. \times 3 = 24)
	A	B	E	
(2a)		1	1	$1 + 1 \times 2 = 3$
(2b)		1	1	$1 + 1 \times 2 = 3$
(2c)		1	1	$1 + 1 \times 2 = 3$
(2d)		1	1	$1 + 1 \times 2 = 3$
(8g)	3	3	3	$3 + 3 + 3 \times 2 = 12$

bare phonon eigenvectors onto the symmetry coordinates, corresponding to different IrReps. The symmetry coordinates can, *e.g.*, be found on the Bilbao Crystallographic Center [6], in its Solid State Theory Applications (SAM) section [7]. Table 1 sums up individual Cartesian displacements of atoms in CZTSe into symmetry coordinates corresponding to IrReps of the space group $I\bar{4}$ (Nr. 82); the corresponding densities of modes are shown in Fig. 2. Of these symmetrized groups of modes, all three are Raman active; B and E are infrared-active. The symmetry coordinates for two-dimensional E modes are for convenience expressed via linear combinations of their respective two partners, that leads to a possible system of symmetry transformations as shown in Table 2 for anions and in

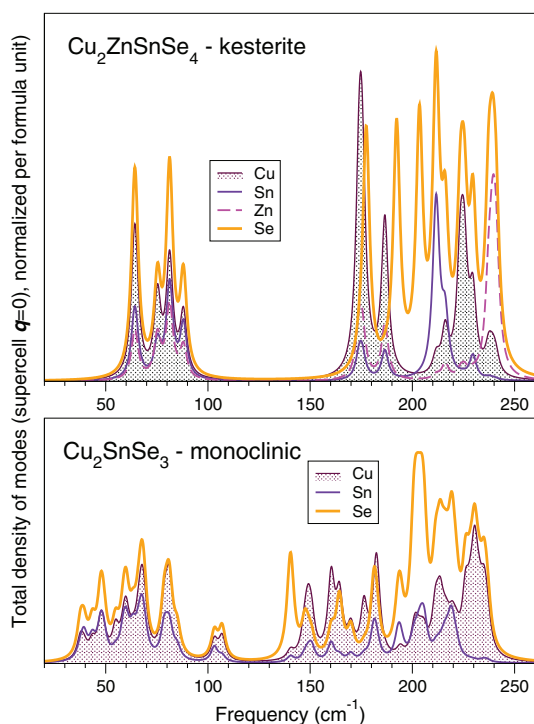


Figure 1 Contribution of different chemical species to zone-center vibration modes in CZTSe (top panel) and CTSe (bottom panel), calculated according to Eq. (1). An artificial smearing of 2 cm^{-1} halfwidth parameter is introduced for better visibility (also in the following figures).

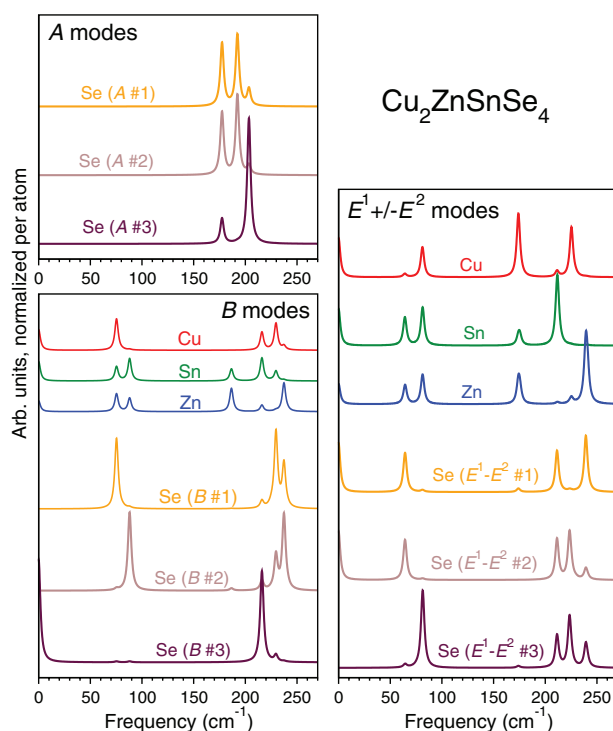


Figure 2 Species-resolved vibration spectra in CZTSe, decomposed according to projections onto A , B , and E IrReps (see Eq. (2)). Note that the decomposition into individual modes within A , B , and E blocks is arbitrary.

Table 2 Symmetry coordinates in different vibration modes constructed from individual Cartesian displacements $\pm(X, Y, Z)$ of anions in CSTSe (space group $I\bar{4}$).

modes	anion sites: $(0\ 0\ 0)^+$; $(\frac{1}{2}\ \frac{1}{2}\ \frac{1}{2})^+$			
	$(\frac{1}{4}\ \frac{3}{4}\ \frac{1}{8})$	$(\frac{3}{4}\ \frac{1}{4}\ \frac{1}{8})$	$(\frac{3}{4}\ \frac{3}{4}\ \frac{7}{8})$	$(\frac{1}{4}\ \frac{1}{4}\ \frac{7}{8})$
A #1	Y	-Y	X	-X
A #2	-X	X	Y	-Y
A #3	-Z	-Z	Z	Z
B #1	Y	-Y	-X	X
B #2	-X	X	-Y	Y
B #3	Z	Z	Z	Z
$(E^1 + E^2)$ 1	X	X	—	—
$(E^1 + E^2)$ 2	Y	Y	—	—
$(E^1 + E^2)$ 3	Z	-Z	—	—
$(E^1 - E^2)$ 1	—	—	Y	Y
$(E^1 - E^2)$ 2	—	—	X	X
$(E^1 - E^2)$ 3	—	—	-Z	Z

Table 3 – for cations. The anions in (8g) positions have three free coordinates (x, y, z) . They are only minutely different from “ideal” high-symmetry positions which we indicate in the header of Table 2 in order to identify the anions. The four remaining “g” sites are obtained by a translation by $\frac{1}{2}\ \frac{1}{2}\ \frac{1}{2}$. As for cation positions, “a” and “c” are occupied by Cu, “b” by Sn, and “d” by Zn.

The (monoclinic) CTSe belongs to the Cc (No. 9) space group; its only (4a) Wyckoff positions, for each of six species (two Cu sites, one Sn, and three Se), are obtained by combining the internal coordinates (x, y, z) ; $x, \bar{y}, z + \frac{1}{2}$ with translations $(0\ 0\ 0)^+$; $\frac{1}{2}\ \frac{1}{2}\ 0^+$. The resulting symmetry coordinates, grouped into two IrReps A' and A'' , are given in Table 4, and the (species-resolved) densities of modes decomposed into A' and A'' are shown in Fig. 3. All modes are both Raman and infrared active.

Tables 2–4 specify, for each IrRep ν , the projection vectors (in the three-dimensional space of individual atom displacements) $\mathcal{S}_i^{\alpha\nu}$ (i : mode index; α : atom index). With these, the symmetry-projected (and species-resolved) density of modes can be recovered as follows:

$$I_{\mathbb{N}}^{\nu}(\omega) = \sum_i \left| \sum_{\alpha \in \mathbb{N}} A_i^{\alpha} \mathcal{S}_i^{\alpha\nu} \right|^2 \delta(\omega - \omega_i). \quad (2)$$

Some remarks concerning these symmetry projections:

- (i) In case of multidimensional IrRep, or when several modes belong to the same symmetry block, the choice

Table 3 Similar to Table 2, for cations.

modes	Wyckoff positions			
	(2a)	(2b)	(2c)	(2d)
B	Z	Z	Z	Z
$(E^1 + E^2)$	X	X	X	X
$(E^1 - E^2)$	Y	Y	Y	Y

Table 4 Symmetry coordinates constructed from individual Cartesian displacements of atoms in CTSe according to A' , A'' IrReps of the Cc space group.

sites	A' modes			A'' modes		
	1	2	3	1	2	3
(x, y, z)	Z	Y	X	-Z	Y	-X
$(x, -y, z + 1/2)$	Z	-Y	X	Z	Y	X

of specific symmetry coordinates is not unique; any their linear combination will do. Hence the projections onto individual symmetrized modes have few physical sense; the sum of squares over modes (or over partners in multidimensional IrRep) should be taken instead.

- (ii) In a calculation done on a unit cell of a perfect compound, there must be a clean separation of vibration modes into different IrReps. In a calculation done with SIESTA method which does not impose any symmetry constraints, a numerical “noise” may spoil this separation somehow. In our calculations, the attribution of each vibration mode to a certain IrRep remained unambiguous. An apparent overlap of the spectra for different IrReps, *e.g.*, in Fig. 3, is due to a dense placement of modes in certain frequency intervals.
- (iii) Zone-center acoustic modes, corresponding to uniform displacement of *all* atoms, must appear in the spectrum; in fact the closeness of their frequencies to zero is an important checkpoint for phonon calculations by SIESTA. Based on the above tables, the symmetry of these modes can be easily identified. For CZTSe, there is one B mode (responsible to the z -uniform displacement) and some two combinations of E^1, E^2 modes (describing displacements in the x, y -plane). Such $\omega = 0$ acoustic modes are well seen in Fig. 2.

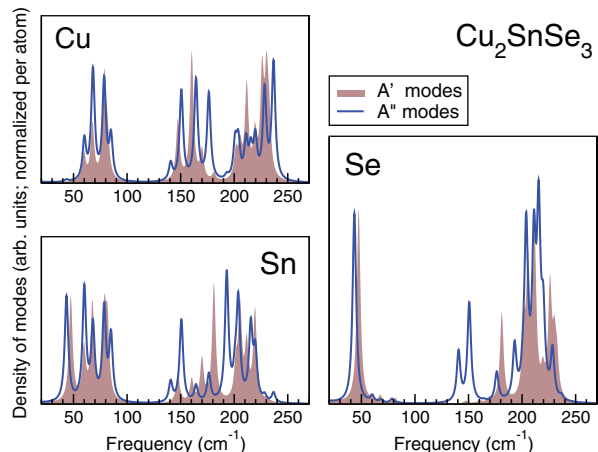


Figure 3 Contribution of different chemical species in vibration modes of CTSe, according to projections corresponding to the A' and A'' IrReps (see Eq. (2)).

2.3 q -resolved modes density; enhancement of $q = 0$ phonons In solid solutions, where topological disorder destroys an exact crystal periodicity, the projection of phonon eigenvectors taken along with a $\exp(i\mathbf{q}\mathbf{R})$ plane wave may help to reveal somehow a smeared $\omega(\mathbf{q})$ dispersion trends in a form of, so to say, spectral function:

$$I_{\mathbb{N}}(\omega, \mathbf{q}) = \sum_i \left| \sum_{\alpha \in \mathbb{N}} A_i^\alpha(\omega) e^{i\mathbf{q}\mathbf{R}_\alpha} \right|^2 \delta(\omega - \omega_i). \quad (3)$$

It amplifies the weights of vibrations in which similar atoms move in phase with a given q -wave throughout the crystal, and suppresses the movements whose phase are at random with such wave. In particular, the $q = 0$ projection amplifies the “prototype” zone-center TO mode of zincblende crystal, the quasi rigid movement of the cation sublattice against the anion one:

$$I_{\mathbb{N}}(\omega, \mathbf{q} = 0) = \sum_i \left| \sum_{\alpha \in \mathbb{N}} A_i^\alpha(\omega) \right|^2 \delta(\omega - \omega_i). \quad (4)$$

In the present case, we do not deal with a solid solution; however, a complex structure (12 cations/12 anions per primitive cell of CTSe) excuses borrowing this tool from our mixed-crystal instrumentary (see Eq. (3) of Ref. [8] and related discussion for such “zone-center insight”).

It turns out that such projection “purifies” the spectrum, reducing it to much better comparable elements shown in Fig. 4. We see now three clearly separated groups of peaks

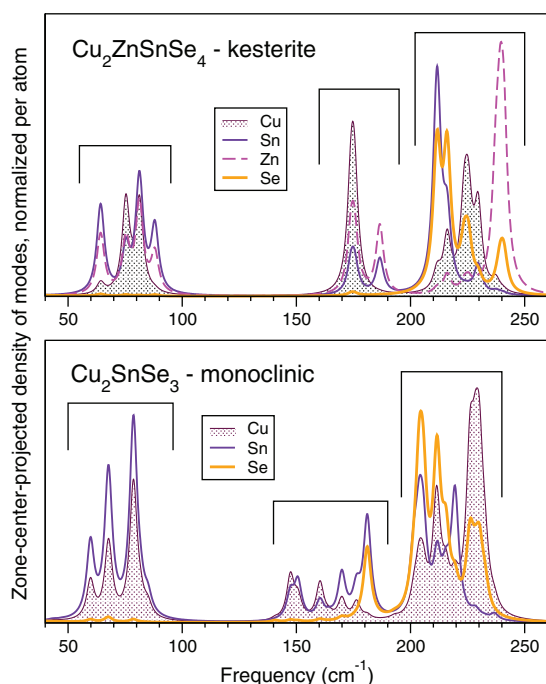


Figure 4 Species-resolved spectra of [zincblende q] = 0 vibration modes in CZTSe and CTSe, calculated according to Eq. (4). For meaning of three groups of peaks, see text.

(instead of two in Fig. 1). Remarkably, the numbering of modes within each group is consistent, in view that CTSe has three times more modes than CZTSe; thus, the throughout numbers of modes in the middle group are 10–13 in CZTSe and 30–39 in CTSe. A detailed analysis group by group and snapshots of characteristic modes can be found in Ref. [3]. In a nutshell, the modes within the softest group are zone-boundary acoustic branches, folded onto zone center of CTSe due to a large unit cell size; the middle group hosts optical modes predominantly stemming from bond bending, and the upper group contains bond-stretching modes. Some modes of CTSe are pronouncedly related to specific structure patterns, in that they “live” on continuous SnSe stripes (planar zigzag chains) or on CuSe chains, both being absent in CZTSe. Certain modes are “twinned”, *i.e.*, a given vibration pattern occurs either in phase, or in counter-phase (but at almost equal frequency) between two identical fragments traversing the same unit cell. For comparison, in CZTSe kesterite the degeneracy of modes occurs exclusively due to $x \leftrightarrow y$ equivalence in the tetragonal structure. Moreover, all cation chains in the kesterite structure are “broken” (*i.e.*, all cations intervene in them in alternation), and no “pure” continuous chains involving only a certain cation occur. One can conclude that the existing difference in vibration spectra are much more due to topological differences (connectivity on the cation sublattice) than to chemical aspect (presence or absence of Zn in the formula).

3 Conclusions With this example we wanted to demonstrate that a combined use of different projection techniques, applied to the bulk of data resulting from a phonon calculation on a large system, may be useful for extracting correlations and underlying essential differences between possibly complex spectra.

Acknowledgements The authors are grateful to Susanne Siebentritt for introducing us into the subject of the secondary phase, and to Olivier Pagès for initial kick towards implementing symmetry projections. Calculations were done using the computer resources of PMMS at the University of Lorraine.

References

- [1] G. Marcano, C. Rincón, L. M. de Chalbaud, D. B. Bracho, and G. Sánchez Pérez, *J. Appl. Phys.* **90**, 1847 (2001).
- [2] N. B. Mortazavi Amiri and A. Postnikov, *Phys. Rev. B* **82**, 205204 (2010).
- [3] N. B. Mortazavi Amiri and A. Postnikov, *J. Appl. Phys.* **112**, 033719 (2012).
- [4] J. M. Soler, E. Artacho, J. D. Gale, A. García, J. Junquera, P. Ordejón, and D. Sánchez-Portal, *J. Phys.: Condens. Matter* **14**, 2745 (2002).
- [5] SIESTA web site, <http://icmab.cat/leem/siesta/>.
- [6] Bilbao crystallographic server, <http://www.cryst.ehu.es/>.
- [7] Go to <http://www.cryst.ehu.es/rep/sam.html>, choose the space group, select a Wyckoff position, select “Show”, go to “Mechanical representation” and again select “Show”.
- [8] O. Pagès, A. V. Postnikov, M. Kassem, A. Chafi, A. Nassour, and S. Doyen, *Phys. Rev. B* **77**, 125208 (2008).